AIChE WILEY InterScience DISCOVER SOMETHING GREAT

FLUID MECHANICS AND TRANSPORT PHENOMENA

Polymer Flocculation of Calcite: Relating the Aggregate Size to the Settling Rate

Alex R. Heath
A.J. Parker Cooperative Research Centre for Hydrometallurgy (CSIRO Minerals), Clayton South, Victoria, Australia

Parisa A. Bahri
A.J. Parker Cooperative Research Centre for Hydrometallurgy (Murdoch University), School of Engineering - Rockingham Campus, Western Australia

Phillip D. Fawell and John B. Farrow
A.J. Parker Cooperative Research Centre for Hydrometallurgy (CSIRO Minerals), Waterford, Western Australia

DOI 10.1002/aic.10789
Published online February 21, 2006 in Wiley InterScience (www.interscience.wiley.com).

The initial hindered settling velocities of flocculated calcite suspensions have been related to the mean aggregate sizes and solid fraction under a range of flocculation conditions that are similar to those occurring within a mineral processing thickener. Calcite particles were flocculated in turbulent pipe flow and the aggregates sized with an in situ *probe (Lasentec FBRM). The flocculated suspension then flowed into vertical column used to measure the hindered settling velocity. This allowed the investigation of key flocculation parameters — the flocculant dosage, the primary particle size, the suspension solid fraction and the fluid shear rate. The hindered settling velocity was related to the mean aggregate size using a relationship based on Richardson and Zaki's extension of Stokes' law. The effect of aggregate porosity was incorporated using fractal geometry, allowing the estimation of the fractal dimension (2.4) from experimental data. It is an important step toward the development of a link between the size of aggregates produced by flocculation, and their settling and dewatering characteristics. This is also an essential step in the development of robust process models describing the performance of gravity thickeners which are widely used throughout the minerals and other industries.*
 AIChE J, 52: 1987–1994, 2006
Keywords: flocculation, settling/sedimentation

Introduction

Particulate settling in viscous fluids has been studied in a range of natural and industrial systems,[1,2,3] with aggregation increasing the settling velocity of fine particles. Natural examples include the formation of river estuary systems when suspended silt is coagulated by the ions dissolved in the seawater,[4] or droplet coalescence in clouds, ultimately producing rain.[5] The action of soluble salts to coagulate and increase the settling of fine particles is exploited in drinking and wastewater treatment plants, typically by adding multivalent cation salts like alum.[6-9] However, in mineral processing circuits coagulants have been largely superseded by high-molecular-weight ($\approx 20 \times 10^6$ g mol^{-1}) polymer flocculants.[10,11]

Particle settling occurs in three distinctly different regimes depending on the effective solid volume fraction. When the solid volume fraction is low, the particles are well separated and settle independently from each other. The gravity sedimen-

Correspondence concerning this article should be addressed to A. R. Heath at alex.heath@csiro.au.

tation velocity of individual solid spheres settling in creeping flow (Re $\rightarrow$ 0) was first described theoretically by Stokes[2,12,13]

$$U = \frac{d^2 g(\rho_s - \rho_l)}{18\mu} \quad (1)$$

where U is settling velocity, m s^{-1}; d is particle diameter m; g is gravity, 9.8 m s^{-2}; ρ is density (s = solid, l = liquid), kg m^{-3}; and μ is fluid viscosity, N s m^{-2}.

In practice, mineral particles/aggregates are rarely spherical, and large aggregates may be highly porous. Nonspherical particles generally settle slightly slower (by a factor of $\sim$ 0.7–1.0) than spheres,[12-16] although needle shaped particles settle slightly faster if the major axis remains vertical. Porous aggregates have larger hydrodynamic profiles than solid particles of the same mass, and the increased drag considerably reduces their settling velocity compared to solid particles of the same size.[17] However, aggregates still settle more rapidly than individual fine particles. Highly porous aggregates may also allow some fluid flow through the structure.[18]

Large, dense particles may settle too rapidly to be accurately described by Stokes' law for viscous flow, and by a particle Reynolds number above about 0.1 inertial effects become significant.[13,19] Both empirical and theoretical functions have been proposed for the drag coefficient at higher Reynolds numbers,[20-23] although in most cases aggregates settle sufficiently slowly to be described by Stokes' law.[17]

As the suspension solid fraction is increased there is a gradual transition to hindered-settling. The hindered settling regime is characterized by a distinct solid/liquid interface (mudline) that settles to leave a clear supernatant above.[24-27] The settling velocity of the mudline decreases as a function of the solid fraction, due to the decreasing permeability of the settling layer and an increase in the upward velocity of the displaced fluid,[23, 28-31] as described by Richardson and Zaki[1]

$$U_h = U_o(1 - \phi)^n \quad (2)$$

where U_h is hindered settling velocity, m s^{-1}; U_o is settling velocity at infinite dilution, m s^{-1}; n is the exponent, $\sim$ 4.65, and ϕ is the solid volume fraction, 0,1.

A wide variety of similar relationships have also been proposed in the literature,[28,30,32] but usually as functions only of the volume fraction, ignoring the effects of flocculation. Of the various hindered settling functions proposed, Richardson and Zaki's equation (Eq. 2) is the most popular, with the exponent typically taken as 4.65.[19,23,33-37,]

Aggregation increases the hindered-settling velocity by increasing the particle size, forming channels in the settling sediment that increase the suspension permeability. Settling behavior in the hindered settling regime is often described with Kynch[29,39] theory, but since the settling velocity is usually taken as a unique function of the solid fraction it does not account for the effect of flocculation[7,40]. In the past this effect was difficult to quantify, because although the hindered settling velocity can be measured relatively easily (for example, by cylinder tests), the fragile aggregates needed to be subsampled for the traditional *ex situ* particle sizing instruments. However, in-stream aggregate sizing instruments are now available,[41] allowing the effect of aggregate size on the hindered settling velocity to be studied directly.

As the solid loading is increased further, the particles will eventually form a continuous network and settling will also be restrained by mechanical support from below.[22,29,36,42,43] The mechanical strength of the network is a function of the solid/packing fraction and the strength of the interparticle bonding. The sediment will compress when the weight of sediment overburden exceeds the compressive yield stress.[31,43-45] The excess overburden weight not supported mechanically is restrained hydrodynamically, and is the force required to squeeze the fluid back up through the collapsing sediment.[46-50] In practice channel formation may occur spontaneously, or can be encouraged by rakes with vertical pickets.[7,29,40,51]

The aim of this work is to develop a mathematical relationship between the aggregate size and the initial hindered settling velocity under a range of conditions likely in a mineral processing thickener. The influence of fluid shear, flocculant dosage, feed solid volume fraction, primary particle size and residence time are addressed. This work continues on from previous studies,[52] where the aggregate size data was used to develop a population balance model describing the kinetics of aggregation and breakage. Hence, a direct link is made between the aggregate size and the corresponding hindered settling velocities of the same suspensions at each stage of the flocculation process.

Experimental

Aggregation of calcite (Omyacarb, Commercial Minerals) with a commercial 30% anionic high-molecular-weight polymer (Nalco 9902) was performed in a linear horizontal pipe reactor, as previously described.[53] The flocculation conditions are summarized in Table 1. Size measurements were taken using the Lasentec FBRM probe,[41] and hindered settling velocities taken in a graduated 0.5 m settling column (Figure 1).

The settling column was constructed from acrylic tube (38.1 mm ID), and the flow was isolatable (note valves in Figure 1) and removable for extended settling measurements. The valve arrangement allowed a portion of the flow to be captured in the settling column, without disrupting the flow through the pipe reactor and past the sizing probe, allowing continuous operation. The column was marked at regular intervals (1 and 5 cm) and lit from behind by a fluorescent tube, allowing the measurement of the hindered settling velocity by following the fall of the mudline through time using a stopwatch.

The pipe work and fittings were designed to keep the top of the settling column as close as possible to the particle-sizing probe, reducing the additional residence time. This was the primary reason for mounting the pipe reactor above floor level (note Figure 1). The fittings around the bend and valve were also constructed to produce a smooth inner surface in an effort to reduce turbulence. Despite this, the reaction time offset between the aggregate size measurement and the top of the settling column was still considerable, requiring a correction (see next section).

Results and Discussion

Effect of fluid shear

Figure 2 shows the development of the mean aggregate size, and corresponding hindered settling velocity as a function of

Table 1. Matrix of Pipe Reactor Experimental Runs

Run No.	Pipe ID (m)	Flow Velocity (m s^{-1})	Solid ϕ (m^3 m^{-3})	Mean d_p (μm)	Floc. Dose (g t^{-1})
1	0.0254	0.461	0.0369	6.59	20.0
2	0.0254	0.461	0.0369	6.59	**40.0**
3	0.0254	0.461	0.0369	6.59	**10.0**
4	0.0254	0.461	0.0369	6.59	**80.0**
5	0.0254	0.461	0.0369	6.59	**5.0**
6	0.0254	0.461	**0.0246**	6.59	20.0
7	0.0254	0.461	**0.0615**	6.59	20.0
8	0.0254	0.461	**0.0123**	6.59	20.0
9	0.0254	0.461	**0.0492**	6.59	20.0
10	0.0254	**0.781**	0.0369	6.59	20.0
11	0.0254	**1.294**	0.0369	6.59	20.0
12	**0.0381**	**0.554**	0.0369	6.59	20.0
13	**0.0381**	**0.343**	0.0369	6.59	20.0
14	**0.0381**	**0.207**	0.0369	6.59	20.0
15	0.0254	0.461	0.0369	**15.08**	20.0
16	0.0254	0.461	0.0369	**2.36**	20.0
17	0.0254	0.461	0.0369	**3.47**	20.0
18	0.0254	0.461	0.0369	**24.26**	20.0
19	0.0254	0.461	**0.0246**	**15.08**	20.0
20	0.0254	**0.781**	0.0369	6.59	**40.0**
21	**0.0381**	**0.343**	0.0369	6.59	**10.0**
22	**0.0381**	**0.343**	**0.0246**	6.59	20.0

Bold face indicates where conditions differ from baseline.

the spatially averaged fluid shear rate and residence time in the pipe. A high turbulent shear rate initially increases the aggregation rate by increasing the mixing and particle collision rates. However, aggregate breakage is also dramatically increased at high shear rates, and larger aggregates are ultimately formed with a lower shear rate. The hindered settling velocity follows a similar trend, but there is a time offset due to the additional pipe-work and fittings between the sizing probe and top of the settling column (Figure 1).

The reaction residence time in the main part of the pipe reactor was taken simply from the mean flow velocity (assuming plug flow), and the distance from the flocculant addition point and the aggregate sizing probe. The additional effective residence time to the top of the settling column was calculated by the velocity-head method,[23] using the Bernoulli equation for incompressible fluids.

The velocity head method was used rather than the simple approach of dividing the volumetric flow rate by the combined volumes of the valve and bend, and so on, because the additional flocculation is a function of both the residence time and the turbulent shear rate. The velocity head is more appropriate and can be converted back to an equivalent number of pipe diameters in the main pipe reactor. Figure 1 shows that in this case several fittings are present between the particle sizing probe and the settling column. The valve on the settling tube was assumed to be fully open with K = 0.17 as suggested by Perry and Green[23]. The protruding sizing probe was also assumed to have K = 0.17, and the tee given as K = 1.0.[23] In addition the expansion loss when using the smaller diameter pipe reactor (25.4 mm ID) was given by the Borda-Carnot equation.[23]

$$\frac{\Delta P}{\rho} = \frac{V_1^2}{2}\left(1 - \frac{A_1}{A_2}\right)^2 \tag{3}$$

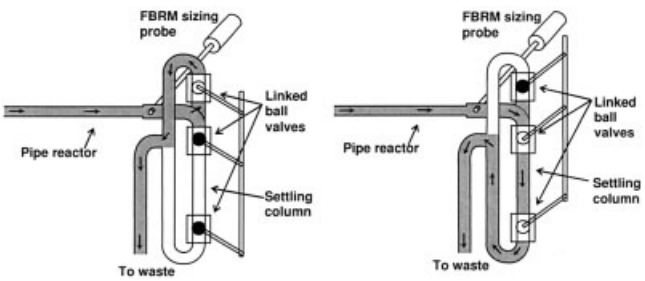

Figure 1. Valve arrangement to capture portion of flow in settling column.

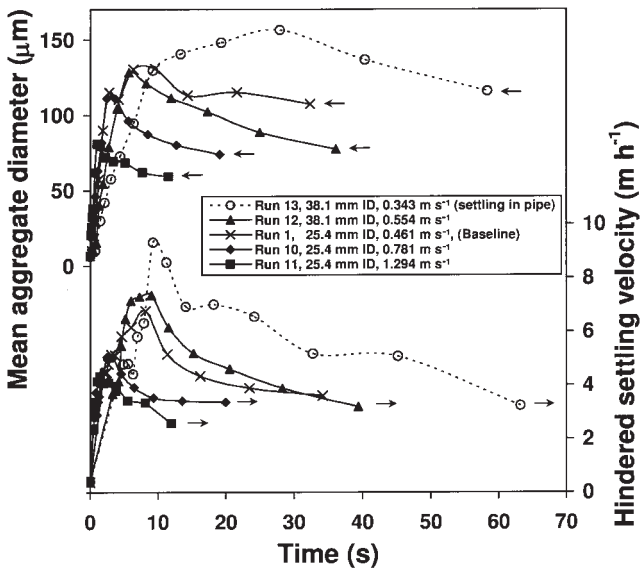

Figure 2. Effect of mean pipe shear rate on the development of the mean aggregate size and hindered settling velocity (other conditions as per baseline).

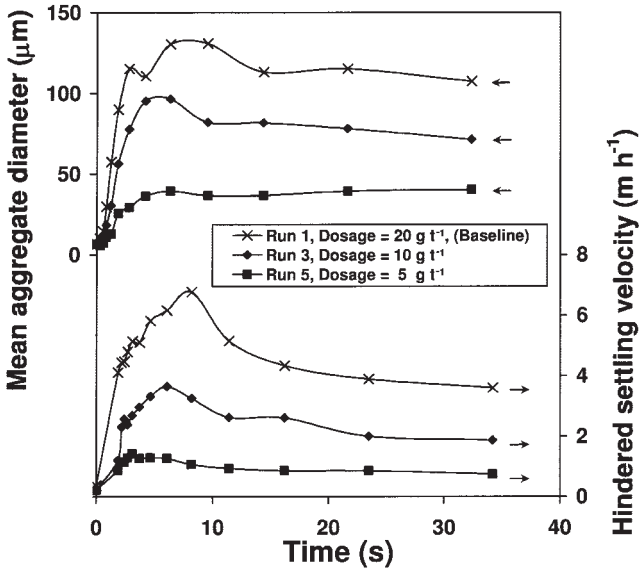

Figure 3. Effect of flocculant dosage on the development of the mean aggregate size and hindered settling velocity (other conditions as per baseline).

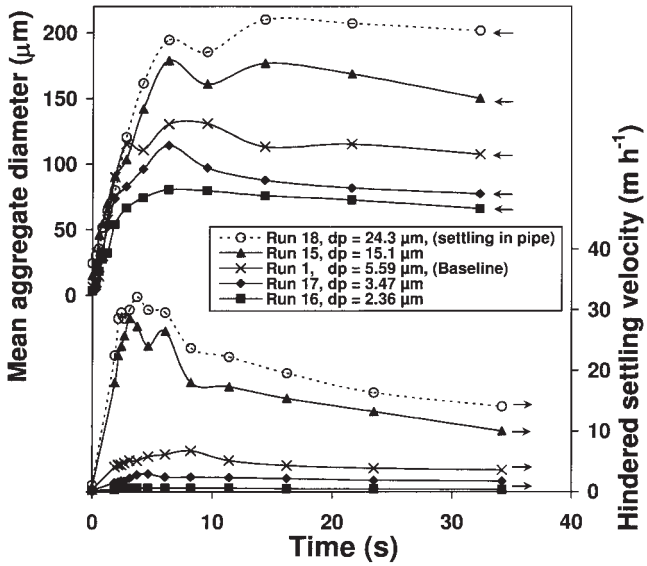

Figure 5. Effect of primary particle size (d_p) on the development of the mean aggregate size and hindered settling velocity (other conditions as per baseline).

where A is cross sectional area of the pipe, m^2.

The contribution from the various fittings and pipe were combined, and converted to an equivalent time depending on the flow velocity and size of the main pipe. The additional equivalent time between the FBRM sizing probe and the top of the settling column varied from 0.44 s (25.4 mm pipe, 39.33 L $min.^{-1}$) to 7.31 s (38.1 mm pipe, 14.16 L $min.^{-1}$), and was added to the x-axis of Figures 2-5. In Figures 3, 4 and 5 below (all with 25.4 mm pipe, 14.01 L $min.^{-1}$) the offset was a constant 1.86 s. The additional time offset is unfortunate, since the data is lost from low-residence times, where the aggregate size increases rapidly. However, it does serve to reinforce the observation that flocculation is rapid in well-mixed suspensions of high-solid fraction.

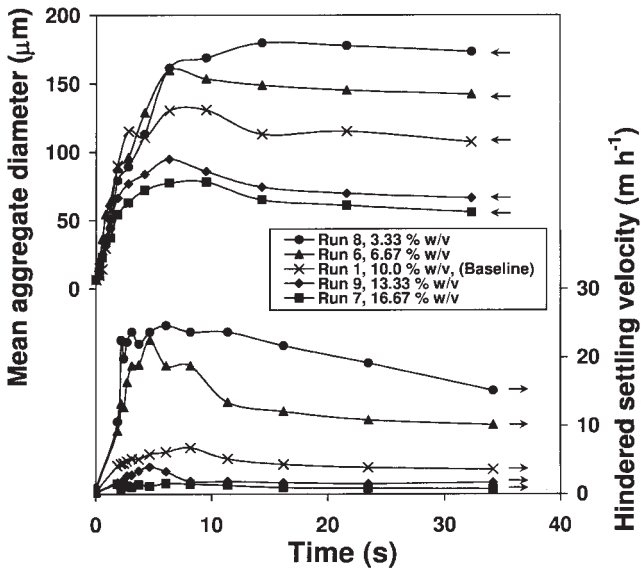

Figure 4. Effect of suspension solid fraction on the development of the mean aggregate size and hindered settling velocity (other conditions as per baseline).

Effect of flocculant dosage

Figure 3 shows the increase in the aggregate size and hindered settling velocity with flocculant dosage. The increased size is attributed to a higher flocculant surface coverage and increased particle bridging,[10] leading to stronger aggregates and a reduced breakage rate. However, repeated aggregation/breakage causes polymer chain scission and/or rearrangement, tending to flatten the polymer chains onto the particle surface and reducing their ability to form polymer bridges between particles. This results in a reduced flocculant activity and the reduction in the aggregate size at extended residence times. If the particles were coagulated, or if charge neutralization (patch model) was the dominant flocculation mechanism, a stable steady-state aggregate size would be produced,[10] where the aggregation and breakage rates were balanced.

Higher flocculant dosages (40 and 80 g t^{-1}) were also tried (not shown), increasing the aggregate size and settling velocity further, however, the increased settling velocity caused the solid to settle to the base of the pipe reactor, invalidating the measurements. Although the flow rate could have been increased, allowing the suspension of larger aggregates formed at a higher flocculant dosage, this would also result in a higher shear rate and increased aggregate breakage (Figure 2).

Effect of suspension solid fraction

Figure 4 shows the effect of the solid fraction on the mean aggregate size and corresponding hindered settling velocity. The decreased size at high-solid fraction is attributed to an increase in fluid viscosity and energy dissipation rate during

flocculation, leading to an increased breakage rate and smaller aggregates. The hindered settling velocity is further reduced by greater hindrance at an increased solid fraction, as described by Eq. 2.

Effect of primary particle size

Figure 5 shows the effect of primary particle size on the aggregate size and subsequent hindered settling velocity. A larger primary particle has a lower surface area (per unit mass) and, hence, a higher flocculant surface coverage. This leads to a stronger aggregate and an increased size due to a reduction in the breakage rate. In addition, a larger primary particle also leads to a lower aggregate porosity (Eq. 6), further increasing the settling velocity.

Fractal geometry

Aggregate porosity is usually described by fractal geometry,[54] where although the total enclosed volume of the aggregate increases as a cube of its diameter, its mass increases at some lower fractional (hence, fractal) power

$$m \propto \left(\frac{d_{agg}}{d_p}\right)^{D_f} \tag{4}$$

where m to aggregate mass kg; d to diameter (agg = aggregate, p = primary particle), m, and D_f to mass-length fractal dimension.

The increase in porosity with aggregate size is usually rationalized on the basis of the increasing voidage produced later in the aggregation process where large aggregates result from aggregate-aggregate collision. Aggregate porosity has two major impacts on the hindered settling velocity. First, it dramatically reduces the aggregate density, reducing the driving force for the particle to settle under gravity (Eq. 1), giving[55-58]

$$(\rho_{agg} - \rho_l) = (\rho_s - \rho_l)\left(\frac{d_{agg}}{d_p}\right)^{D_f-3} \tag{5}$$

where ρ is density (s = solid, l = liquid, agg = aggregate), kg m^{-3}.

Second, the effective suspension solid volume fraction is increased, increasing the inter-particle hindrance as described by Richardson and Zaki[1,59,60] (Eq. 2)

$$\phi_{eff} = \phi_s\left(\frac{d_{agg}}{d_p}\right)^{3-D_f} \tag{6}$$

where ϕ is the solid volume fraction (s = solid, eff = effective) [0,1].

Combining Eqs. 1, 2, 5 and 6, and substituting mean sizes gives

$$U_h = \frac{\overline{d_{agg}^2}g(\rho_s - \rho_l)\left(\frac{\overline{d_{agg}}}{\overline{d_p}}\right)^{D_f-3}}{18\mu}\left(1 - \phi_s\left(\frac{\overline{d_{agg}}}{\overline{d_p}}\right)^{3-D_f}\right)^{4.65} \tag{7}$$

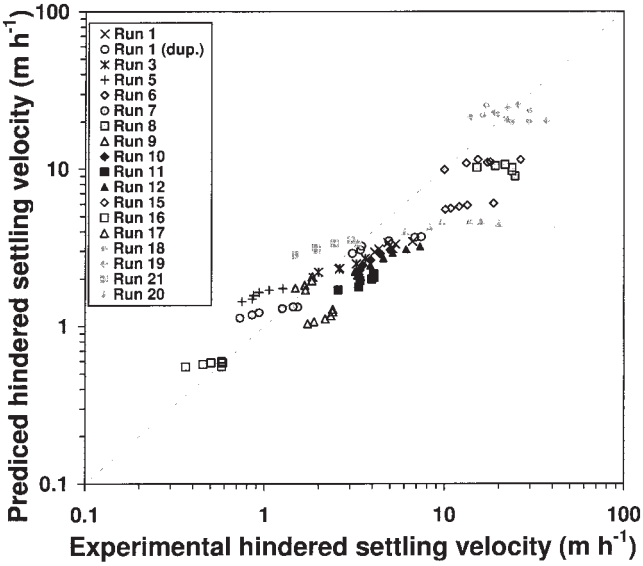

Figure 6. Comparison between measured and predicted (Eq. 7) hindered settling velocities.

The settling velocity may be further reduced by the effect of particle shape as the particles deviate from the sphericity assumed by the earlier equations. However, the effect of shape is relatively minor at low-particle Reynolds number ($\sim$ 0.7–1.1 times the rate[12-16]), and is partially offset by the permeability of porous aggregates, allowing some fluid flow through the structure, decreasing the drag slightly.[17,18] Hence, the effects of particle shape, permeability, and Reynolds' number have been ignored as unnecessary complications at this stage, and Eq. 7 incorporates the dominant effects (suspension solid fraction and aggregate density) into the Stokes' Equation to predict the hindered settling velocity.

In this case the fluid viscosity is taken to be a constant 0.00102 N s m^{-2} (water at 20 °C[61]), and is unaffected by the aggregation process. During hindered settling the particles are essentially joined together as a continuous, permeable network, with the displaced water passing through channels in the sediment. Equation 7 was used to estimate the fractal dimension (D_f) from the experimental data via

$$\min_{D_f} = \sum_{G,\phi,\theta,d_p,t}\left(\frac{U_{h,Exp} - U_{h,Eq.7}}{U_{h,Exp}}\right)^2 \tag{8}$$

where $U_{h,\mathrm{Exp}}$ is the experimental hindered settling velocity, m s^{-1}; U_h ,(Eq. 7) is the predicted hindered settling velocity from Eq. 7, m s^{-1}.

In this case the fractal dimension (D_f) was found to produce the best fit with a value of 2.42 (Figure 6), which is a typical value for aggregates formed by flocculation at high shear rates.[62-66]

Aggregate settling data typically displays considerable scatter (perhaps due to shape effects), however, a sensitivity analysis was performed to determine if the fractal dimension (D_f) was a function of any of the experimental variables (shear rate G, flocculant dosage θ, primary particle size d_p and solid

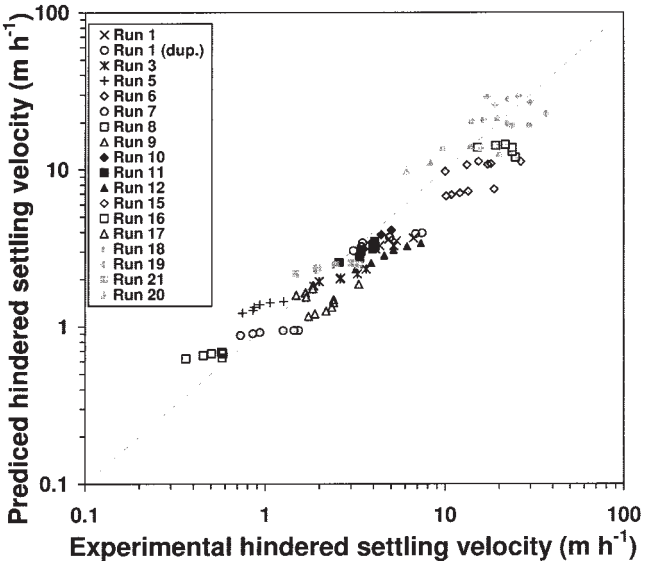

Figure 7. Comparison between measured and predicted (Eqs. 7 and 9) hindered settling velocities.

fraction ϕ). Both linear and nonlinear sensitivities were tried as per Eqs. 12 and 13, the linear according to

$$D_f = D_f^* + A\left(\frac{G_{Exp} - G_{BL}}{G_{BL}}\right) + B\left(\frac{\theta_{Exp} - \theta_{BL}}{\theta_{BL}}\right) + C\left(\frac{d_{p,Exp} - d_{p,BL}}{d_{p,BL}}\right) + D\left(\frac{\phi_{Exp} - \phi_{BL}}{\phi_{BL}}\right) \quad (9)$$

With G to the mean shear rate, s^{-1}; θ is the flocculant dosage, kg m^{-2}; d_p is the Primary particle size (m); ϕ is the solid fraction [0,1]; *Exp* is the experimental condition; *BL* is the experimental condition at baseline $D_f^* = 2.43$; $A = 0.0244$; $B = 0.0842$; $C = -0.0060$; $D = 0.0786$, and the nonlinear

$$D_f = D_f^*\left(\frac{G_{Exp}}{G_{BL}}\right)^w\left(\frac{\theta_{Exp}}{\theta_{BL}}\right)^x\left(\frac{d_{p,Exp}}{d_{p,BL}}\right)^y\left(\frac{\phi_{Exp}}{\phi_{BL}}\right)^z \quad (10)$$

With $D_f^* = 2.44$; $W = 0.01949$; $X = 0.0337$; $Y = 0.00314$, and $Z = -0.0337$.

Figure 7 shows the fit using the linear method (Eq. 9), with the residual reduced from 19.4 (Figure 6) to 11.9. The nonlinear method (not shown, Eq. 10) reduced the residual fractionally further, to 10.5. The improvement of Figure 7 over Figure 6 is minor, considering the number of degrees of freedom increased from 1 to 5, indicating that Equation 7 holds reasonably well within the experimental scatter.

The sensitivity analysis indicates some increase in the fractal dimension (less porous) with shear and flocculant dosage, but a decrease with solid fraction. However, caution may be required interpreting these observations, since none of the effects are very strong (that is, $D_f \approx 2.4 \pm 0.1$), and do not change the overall observation that the initial hindered settling velocity is increased with flocculant dosage (Figure 3), and primary particle size (Figure 5), but decreased with solid fraction (Figure 4) and shear rate (Figure 2).

Figures 2, 3, 4, and 5 show a slight reduction in aggregate size on extended shearing, typical of aggregates formed by polymer flocculants.[10,67-69] This effect could be interpreted as either aggregate compaction, or partially irreversible breakage (or both).[57,64,70] However, aggregate breakage appears to be the dominant mechanism for this system, because in all cases the hindered settling velocities also drop with aggregate size on extended shearing. If compaction was the dominant size reduction mechanism, the hindered settling velocity would be expected to rise due to the increased density (Eq. 5), and reduced effective solid fraction (Eq. 6).

Conclusions

The initial hindered settling velocities of flocculated calcite suspensions have been studied under various process conditions (fluid shear, flocculant dosage, primary particle size, solid fraction) and related to on-line aggregate size measurements. As would be expected a larger aggregate size leads to a higher hindered settling velocity, however, the effects of inter-particle hindrance must also be considered. Richardson and Zaki's[1] relationship describing the hindered settling velocity of non-flocculated suspensions has been adapted to flocculated suspensions by incorporating fractal geometry to describe aggregate porosity. This has enabled the estimation of the fractal dimension (2.4) from the experimental data.

Acknowledgments

This research has been supported by the Australian Government's Cooperative Research Centre (CRC) program, through the AJ Parker CRC for Hydrometallurgy. Considerable support was also provided by the industrial sponsors of the AMIRA P266C Improving Thickener Technology project. This support is gratefully acknowledged.

Notation

A = cross sectional area of the pipe, m^2
BL = subscript, experimental condition at baseline
d = particle dia., m
d_p = diameter of primary particle, m
d_{agg} = diameter of aggregate, m
D_f = mass-length fractal dimension
Exp = subscript, experimental condition
g = gravity, m s^{-2}
G = mean shear rate, s^{-1}
m = aggregate mass, kg
n = exponent in Eq. 2, usually taken as 4.65
ΔP = pressure drop, N m^{-2}
U = settling velocity, m s^{-1}
U_o = settling velocity at infinite dilution, m s^{-1}
U_h = hindered settling velocity m s^{-1}
$U_{h,\mathrm{Eq.7}}$ = predicted hindered settling velocity from Eq.7, m s^{-1}
$U_{h,\mathrm{Exp}}$ = experimental hindered settling velocity, m s^{-1}
V = mean fluid velocity, m s^{-1}
ρ_s = density of solid, kg m^{-3}
ρ_l = density of liquid, kg m^{-3}
ρ_{agg} = density of aggregate, kg m^{-3}
θ = flocculant dosage, kg m^{-2}
ϕ = solid volume fraction, 0,1
ϕ_s = solid volume fraction, excluding aggregate porosity, 0,1
ϕ_{eff} = effective solid volume fraction, including aggregate porosity, 0,1
μ = fluid viscosity, N s m^{-2}

Literature Cited

1. Richardson JF, Zaki WN. Sedimentation and fluidisation. *Trans Instn Chem Engrs*. 1955;32:35-53.
2. Stokes GG. On the effect of the inertial friction of fluids on the motion of pendulums. *Trans Cambridge Philos Soc*. 1851;9:8-106.

3. Tory EM. *Sedimentation of Small Particles in a Viscous Fluid*. Glasgow: Bell & Bain Publishers; 1996.
4. Stumm W, Morgan JJ. *Aquatic Chemistry*. 3rd ed. New York: Wiley-Interscience; 1996.
5. Saffman P, Turner J. On the collision of drops in turbulent clouds. *J of Fluid Mechanics*. 1956;1:16-30.
6. Amirtharajah A, Clark MM, Trussell RR. *Mixing in Coagulation and Flocculation*. USA: American Water Works Association Research Foundation; 1991.
7. Williams RA. *Colloid and Surface Engineering, Applications in the Process Industries*. UK: Butterworth-Heinmann; 1992.
8. Kohler HH. Thermodynamics of Adsorption from solution. In: Dobias B. *Coagulation and Flocculation: Theory and Applications*. New York: Marcel Dekker; 1993.
9. Hughes MA. Coagulation and Flocculation. In: Svarovsky L. *Solid-Liquid Separation*. 4th ed. UK: Butterworth-Heinmann; 2000.
10. Bagster DF. Aggregate behaviour in stirred vessels. In: Shamlou PA. *Processing of Solid-Liquid Separations.* UK: Butterworth-Heinemann, Ltd., 1993;26-58.
11. Farinato RS, Dubin PL. *Colloid-Polymer Interactions, From Fundamentals to Practice*. UK: John-Wiley & Sons; 1999.
12. Happel J, Brenner H. The motion of a rigid particle of arbitrary shape in unbounded fluid. Chapter 5 in: *Low Reynolds Number Hydrodynamics*. Leyden: Noordhoff International Publishing; 1973.
13. Seville JPK, Tüzün U, Clift R. *Processing Particulate Solids*, Melbourne: Blackie Academic & Professional; 1997.
14. Pettyjohn ES, Christiansen EB. Effect of particle shape on free-settling rates of isometric particles. *Chem Eng Prog*. 1948;44:157-172.
15. Heiss JF, Coull J. The effect of orientation and shape on the settling velocity of non-isometric particles in a viscous medium. *Chem Eng Process*. 1952;48:133-140.
16. Kousaka Y, Okuyama K, Payatakes AC. Physical meaning and evaluation of dynamic shape factor of aggregate particles. *J of Colloid and Interface Sci*. 1981;84:91-99.
17. Gregory J. The role of floc density in solid-liquid separation. *Filtration and Separation*. 1997;35:367-371.
18. Veerapaneni S, Wiesner MR. Hydrodynamics of fractal aggregates with radially varying permeability. *J of Colloid and Interface Sci*. 1996;177:45-57.
19. Rushton A, Ward AS, Holdich RG. *Solid-Liquid Filtration and Separation Technol*. Germany: VCH, 1996.
20. Moudgil BM, Vasudevan TV. Evaluation of floc properties for dewatering fine particle suspensions. *Minerals and Metallurgical Processing*. 1989;6:142-145.
21. Clift R, Grace JR, Weber ME. *Bubbles, Drops and Particles*. New York: Academic Press; 1978.
22. Nguyen-Van A, Schulze HJ, Kmet S. A simple algorithm for the calculation of the terminal velocity of a single solid sphere in water. *Int J of Min Proc.* 1994;41:305-310.
23. Perry HR, Green DW. *Perry's Chemical Engineers' Handbook*. 7th ed. McGraw-Hill; 1997.
24. Bhatty JI, Davies L, Dollimore D. The use of hindered settling data to evaluate particle size or floc size, and the effect of particle-liquid association on such sizes. *Surface Technol.* 1982;15:323-344.
25. Fitch B. Current theory and thickener design - Part 1, Introduction - zone settling theories. *Filtration and Separation*. July 1975. 1975;355-359.
26. Fitch EB. Gravity sedimentation operations. In: McKetta JJ, Cunningham WA. *Encyclopedia of Chemical Processing and Design*. New York: Marcel Dekker; 1987;25.
27. Tong P, Basu A, Alexander KS, Dollimore D. Development of a new theory for hindered settling suspensions. *STP Pharma Sci*. 1998;8:241-247.
28. Govier GW, Aziz K. *The Flow of Complex Mixtures in Pipes.* Melbourne: Van Nostrand Reinhold Company. 1972.
29. Pearse MJ. *Gravity Thickening Theories: A Review*. UK: Warren Spring Laboratory, Dept. of Industry; 1977.
30. Williams RA, Amarasinghe WPK. Measurement and simulation of sedimentation behaviour of concentrated polydisperse suspensions. *Trans Instn Min Metall.* 1989;98;C68–C82.
31. Bustos MC, Concha F, Burger R, Tory EM. *Sedimentation and Thickening*. London: Kuwer Academic Publishers; 1999.
32. Famularo J, Happel J. Sedimentation of dilute suspensions in creeping flow. *AIChE J*. 1965;11:981-988.
33. Davis RH, Gecol H. Hindered settling function with no empirical parameters for polydisperse suspensions. *AIChE J*. 1994;40:570-575.
34. Kanungo SB, De PK. Physico-chemical studies of precipitated magnesium hydroxide: part III - estimation of floc characteristics from hindered settling rates of dilute suspensions. *Indian J of Technol*. 1970;8:180-184.
35. Maude AD, Whitmore RL. A generalized theory of sedimentation. *Br J Appl Phys*. 1958;9:477-482.
36. Michaels AS, Bolger, JC. Settling rates and sediment volumes of flocculated kaolin suspensions. *I&EC Fundamentals*. 1962;1:24-33.
37. Turian RM, Ma TW, Hsu FLG, Sung DJ. Characterization, settling, and rheology of concentrated fine particulate mineral slurries. *Powder Technol*. 1997;93:219-233.
38. Di Felice R. Solid suspension in liquid fluidised beds. In: Shamlou PA. *Processing of Solid-Liquid Separations.* UK: Butterworth-Heinemann, Ltd.; 1993
39. Kynch GJ. A theory of sedimentation. *Trans Faraday Soc*. 1952;48: 166-176.
40. Svarovsky L. *Solid-Liquid Separation.* 4th ed. UK: Butterworth-Heinmann; 2000
41. Heath AR, Fawell PD, Bahri PA, Swift JD. Estimating average particle size by focussed beam reflectance measurement (FBRM). *Particle and Particle Systems Characterisation*. 2002;9:84-95.
42. Chandler S, Hogg R. Sedimentation and consolidation in destabilised suspensions. *Flocculation in Biotechnology and Separation Systems*. Amsterdam: Elsevier; 1987;279-296.
43. Healy TW, Boger DV, White LR, Leong YK. Scales PJ. Thickening and clarification; how much do we really know about dewatering? *AusIMM Extractive Metallurgy Conference*: Australia; Brisbane; 3-6 July. 1994;105-109.
44. Buscall R, White LR. The consolidation of concentrated suspensions. *Chem Soc Faraday Trans I*. 1987;83:873-891.
45. Green MD, Eberl M, Landman KA. Compressive yield stress of flocculated suspensions: determination via experiment. *AIChE J*. 1996; 42:2308-2318.
46. Fitch B. Current theory and thickener design (1975) - Part 2, Compression theory. *Filtration and Separation*. September/October 1975. 1975;480-553.
47. Wakeman RJ, Holdich RG. Theoretical and experimental modelling of solids and liquid pressures in batch sedimentation. *Filtration and Separation*. Downington; 1984;420-422.
48. Concha F, Bustos MC, Barrientos A. Phenomenological theory of sedimentation. In: Tory EM. *Sedimentation of Small Particles in a Viscous Fluid*. Boston: Computational Mechanics Publications; 1996.
49. Diplas P, Papanicolaou AN. Batch analysis of slurries in zone settling regime. *J of Environ Eng.* 1997;123:659-667.
50. Perez M, Font R, Pastor C. A mathematical model to simulate batch sedimentation with compression behaviour. *Computers Chem Eng*. 1998;22;1531-1541.
51. Dahlstrom DA, Fitch EB. Thickening. In: Weiss, N.L. *SME Mineral Processing Handbook*, American Institute of Mining, Metallurgical, and Petroleum Engineers, Inc. New York: Kingsport Press; 1985.
52. Heath AR, Bahri, PA, Fawell PD, Farrow JB. Polymer flocculation of calicite: Population balance model. *AIChE J.* in press. May 2006.
53. Heath AR, Bahri PA, Fawell PD, Farrow JB. Aggregation of calcite by polymeric flocculant: experimental observations in turbulent pipe flow. *AIChE J.* in press. April 2006.
54. Meakin P. Fractal aggregates. *Adv Colloid Interface Sci.* 1988;28:249-331.
55. Gonzalez EA, Hill PS. A method for estimating the flocculation time of monodispersed sediment suspensions. *Deep-Sea Research*. 1998; 45:1931-1954.
56. Atteia O. Evolution of size distributions of natural particles during aggregation: modelling versus field results. *Colloids and Surfaces A - Physicochem and Eng Aspects*. 1998;139:171-188.
57. Ellis CE, Glasgow LA. Deformability and breakage of flocs. *Advances in Environ Res*. 1999;3:15-27.
58. Manning AJ, Dyer KR. A laboratory examination of the floc characteristics with regard to turbulent shearing. *Marine Geology*. 1999;160: 147-170.
59. Potanin AA, Uriev NB. Microrheological models of aggregated suspensions in shear flow. *J of Colloid Interface Sci*. 1991;142:385-395.
60. Flesch JC, Spicer PT, Pratsinis SE. Laminar and turbulent shear-

induced flocculation of fractal aggregates. *AIChE J*. 1999;45:1114-1124.
61. Daugherty RL, Franzini JB, Finnemore EJ. *Fluid Mechanics with Engineering Applications*. Singapore: McGraw-Hill; 1989.
62. Jiang Q, Logan BE. Fractal dimensions of aggregates determined from steady-state size distributions. *Environ Sci Technol*. 1991;25:2031-2038.
63. Kusters KA, Wijers JG, Thoenes D. Aggregation kinetics of small particles in agitated vessels. *Chem Eng Sci*. 1997;52:107-121.
64. Oles V. Shear-induced aggregation and breakup of polystyrene latex particles. *J of Colloid Interface Sci*. 1992:154:351-358.
65. Serra T, Casamitjana X. Effect of the shear and volume fraction on the aggregation and breakup of particles. *AIChE J*. 1998;44:1724-1730.
66. Spicer PT, Pratsinis SE, Raper J, Amal R, Bushell G, Meesters G. Effect of shear schedule on particle size, density, and structure during flocculation in stirred tanks. *Powder Technol.* 1998;97:26-34.
67. Keys RO, Hogg R. Mixing problems in polymer flocculation. *Water 1978, AIChE Symposium Series*. 1978;63-72.
68. Pelton RH. A model for flocculation in turbulent flow. *Colloids Surf*. 1981;2:277-291.
69. Williams RA, Peng SJ, Naylor A. *In situ* measurement of particle aggregation and breakage kinetics in a concentrated suspension. *Powder Technol*. 1992;73:75-83.
70. Mills PDA, Goodwin JW, Grover BW. Shear field modification of strongly flocculated suspensions - aggregate morphology. *Colloid Polymer Sci*. 1991;269:949-963.

Manuscript received Jun. 13, 2005, and revision received Jan. 5, 2006.